NEW ADAPTIVE SLIDING-MODE OBSERVER DESIGN FOR SENSORLESS CONTROL OF PMSM IN ELECTRIC VEHICLE DRIVE SYSTEM

Xiong Xiao, Yongjun Zhang*, Jing Wang and Haiping Du
Engineering Research Institute Department
School of University of Science and Technology Beijing
Beijing, China
Emails: zhangyj@ustb.edu.cn

Submitted: Nov. 27, 2015 ***Accepted: Jan. 24, 2016*** ***Published: Mar. 1, 2016***

Abstract- In this study, a new adaptive sliding-mode observer is proposed to estimate the rotor position and speed for sensorless control of permanent-magnet synchronous motor (PMSM) in an electric vehicle drive system. This observer can effectively reduce the estimation errors caused by the inherent chattering phenomenon for a conventional sliding-mode observer and the stator resistance uncertainty due to the variation of motor temperature. This new sliding-mode observer is designed by using a hyperbolic tangent function instead of sign function together with a variable boundary layer, and the new adaptive law is constructed according to the back electromotive force model to reinforce dynamic performance and the robustness of system. Meanwhile, a stator resistance identification algorithm is raised and guaranteed to be stable by using a Lyapunov method. The performance of the developed observer is compared with the conventional sliding-mode controller. Both simulation and experimental results confirm that the chattering phenomenon is effectively eliminated and the estimation accuracy for position and velocity is apparently improved when applying the developed observer in the electric vehicle drive system.

Index terms*: PMSM, adaptive sliding-mode observer, sensorless control, electric vehicle drive system, resistance identification.*

I. INTRODUCTION

Electric vehicle (EV) has gained tremendous attention from the past decade as one of the promising greenhouse gasses (GHG) solution and the new direction of the car with energy development [1-3]. Motor drive systems are the core components of electric vehicles and the energy efficiency, high performance, and light weight design are becoming the primary research topics. PMSM has been the best-case scenario in electric vehicle drive system due to its simple structure, small volume, high power factor, small inertia and fast dynamic response [4], [5].

In rotor flux orientation control, how to obtain the rotor position and speed signals, which are traditionally measured by the mechanical and electrical sensors, is a key issue for high performance vector control. However, the installation and debugging of the position transducer will result in high cost and large size of drives and limit the application of PMSM in relatively harsh environment [6]. Therefore, sensorless control of PMSM has been a hot research topic of motor control technology with advantages of low cost and high reliability [7], [8].

Currently, the main methodologies applied to the identification of PMSM speed and estimation of rotor position are categorized into the following classes: basic electromagnetic relation based estimation method [9], [10], model reference adaptive system [11-14], high-frequency injection method [15-19], and nonlinear control theory based method [20-23]. The estimation method based on observer requires high accuracy of motor parameters, which are actually sensitive to measurement noise. Industrial application of high frequency signal injection method is difficult to be realized due to complexity of filter design and is limited by computing speed of controller. Given the above-mentioned circumstances, the sliding-mode observer method is widely used in the speed sensorless control of PMSM system due to its simple structure, rapid response, and good performance of engineering appliance [24], [25].

In order to eliminate the chattering phenomenon in a conventional sliding-mode observer (SMO) with a sign function [26], [27], a low pass filter for high frequency signal filtering and an additional phase compensation of the rotor are introduced, which typically add undesirable level of cost and complexity to the system [28]. Another way to cope with this problem is to apply the approach called “higher order sliding mode” by acting on higher order time derivatives of the sliding manifold, instead of influencing the first time derivative, which improves the controller performance and attenuates the chattering effect to some extent [29]. Moreover, stator resistance

value is required for a stator flux and electromotive force estimation. Its variations caused by changing temperature make operation difficult, mainly at low speed [30]. To overcome this problem, a reduced order extended Kalman filter (EKF) is proposed to update online the stator resistance [31]. A very simple identification algorithm using d-axis stator current error for identifying the stator resistance is also proposed in [32]. A new mode flux observer is presented in [33] with two distinct features: a sliding mode voltage mode flux observer and a fuzzy model reference learning controller. However in these works, all of the methods rely on stator current measurement and predominantly require information regarding stator voltages as well, and the authors also calculate the rotor flux vector angular position in an open loop using the slip estimate which is very sensitive to the parameter uncertainties.

Based on the above literature review, this paper proposes a new SMO for sensorless control of PMSM. In order to remove the chattering problem, the conventional SMO sign function is replaced by the hyperbolic tangent function with variable boundary layer thickness. A novel adaptive law for rotor position and speed estimation is designed by the observer convergence condition. Also, to reduce the influence of the velocity parameter identification precision caused by stator resistance variation, the stator resistance online identification algorithm is proposed based on the Lyapunov stability analysis. Both simulation and experimental results prove that the developed method shows more superior performance compared with the conventional SMO.

This paper is organized as follows. Section 2 discuss about the conventional SMO design for PMSM. Section 3 contains the adaptive SMO presented for the rotor position estimation and stator resistance online identification. In Section 4, the simulation and experimental data from a test rig is used to validate the proposed algorithm, and finally the conclusion closes the paper in Section 5.

II. SLIDING MODE OBSERVER FOR PMSM

a. Modeling of the PMSM

PMSM is a typical nonlinear, multi-variable coupled system, and it is also influenced by many nonlinear factors. For simplicity, we usually make the following assumptions:

1) The motor iron core saturation is ignored;
2) The motor of hysteresis losses and eddy-current losses are not considered;
3) The stator current is symmetrical three-phase sinusoidal wave current;

4) The rotor does not have damping windings.

The electrical and mechanical equations of the PMSM in the rotor reference (αβ) frame is expressed as follows

$$\begin{cases} \dot{i}_\alpha = -\dfrac{R}{L} i_\alpha + \dfrac{1}{L} v_\alpha - \dfrac{1}{L} e_\alpha \\ \dot{i}_\beta = -\dfrac{R}{L} i_\beta + \dfrac{1}{L} v_\beta - \dfrac{1}{L} e_\beta \end{cases} \quad (1)$$

where $i_{\alpha\beta}$, $e_{\alpha\beta}$ and $v_{\alpha\beta}$ represent the current, electromotive force (EMF), and voltage for each phase, R and L represent the stator resistance and inductance, respectively.

The EMF equations of the PMSM is expressed as follows

$$\begin{cases} e_\alpha = -\varphi_f \omega_r \sin\theta \\ e_\beta = \varphi_f \omega_r \cos\theta \end{cases} \quad (2)$$

where φ_f, ω_r and θ represent the flux linkage of the permanent magnet, the motor angular velocity and angle.

b. Conventional SMO Design

According to the basic theory of sliding mode variable structure control and the mathematical model of PMSM, the structure of the stator current sliding-mode observer is expressed as follows

$$\begin{cases} \dot{\hat{i}}_\alpha = -\dfrac{R}{L} \hat{i}_\alpha + \dfrac{1}{L} v_\alpha - \dfrac{1}{L} u_\alpha \\ \dot{\hat{i}}_\beta = -\dfrac{R}{L} \hat{i}_\beta + \dfrac{1}{L} v_\beta - \dfrac{1}{L} u_\beta \end{cases} \quad (3)$$

In (3), u can be represented as

$$\begin{cases} u_\alpha = k_{sw} sign\left(\hat{i}_\alpha - i_\alpha\right) \\ u_\beta = k_{sw} sign\left(\hat{i}_\beta - i_\beta\right) \end{cases} \quad (4)$$

where k_{sw} and $sign(x)$ represent the sliding mode observer gain and the switching function, respectively.

The sliding surface can be defined as

$$S_n = \begin{bmatrix} s_\alpha & s_\beta \end{bmatrix}^T = \begin{bmatrix} \hat{i}_\alpha - i_\alpha & \hat{i}_\beta - i_\beta \end{bmatrix}^T \quad (5)$$

where $s_\alpha = \bar{i}_\alpha$, $s_\beta = \bar{i}_\beta$.

When the system reaches the sliding surface ($S_n = 0$), namely we have

$$\begin{cases} \hat{i}_\alpha = i_\alpha \\ \hat{i}_\beta = i_\beta \end{cases} \quad (6)$$

When satisfying the accessibility of the system gain condition, the system will enter the sliding mode in finite time. According to the theory of equivalent control, we have

$$\begin{cases} (e_\alpha)_{eq} = (u_\alpha)_{eq} \\ (e_\beta)_{eq} = (u_\beta)_{eq} \end{cases} \quad (7)$$

Equation (4) shows that real voltage signals which are derived from the high frequency switch of the current error may comprise the electromotive force information and high-frequency noise part. To this end, the first-order low-pass filter is adopted to filter the high frequency signal, but it also brings the corner phase deviation problem. So we need the phase compensation to be added in the conventional SMO. Fig.1 shows the block diagram of the conventional SMO.

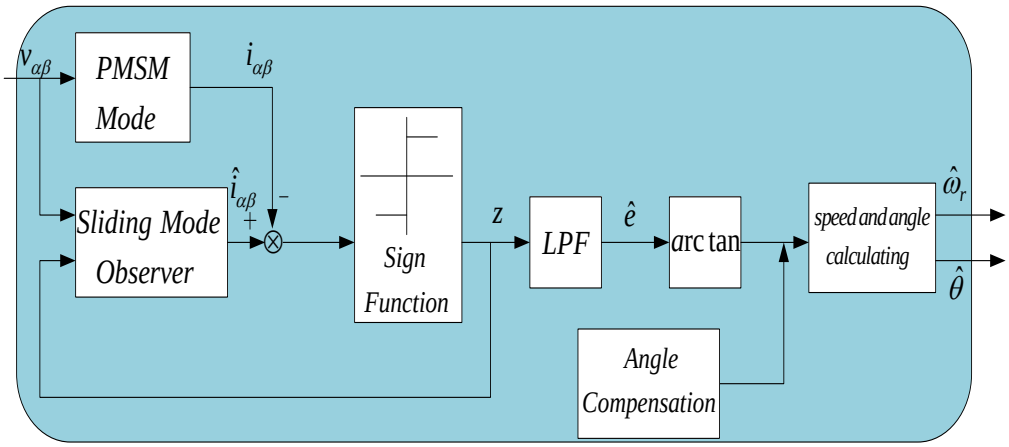

Figure 1. The block diagram of the conventional SMO

III. NEW ADAPTIVE SMO DESIGN

Traditional SMO uses the sign function as a switching function, but the switching with sign function can cause system chattering, which becomes more severe with the rotor velocity increasing. To remove the chattering phenomenon, a continuous switching function, hyperbolic tangent function, is suggested here for a new SMO design without requiring the low pass filter or the extra compensator for the rotor position estimation. On the basis of the new function, the new adaptive law is constructed according to the back electromotive force model to reinforce dynamic performance and the robustness of system. Meanwhile, considering that resistance parameters vary with motor temperature, we design a new stator resistance online identification algorithm based on the Lyapunov stability analysis.

a. Modeling of the PMSM

The structure of the new sliding-mode observer equations is expressed as follows

$$\begin{cases} \dot{\hat{i}}_\alpha = -\dfrac{\hat{R}}{L}\hat{i}_\alpha + \dfrac{1}{L}v_\alpha - \dfrac{1}{L}E\left(\bar{i}_\alpha\right) \\ \dot{\hat{i}}_\beta = -\dfrac{\hat{R}}{L}\hat{i}_\beta + \dfrac{1}{L}v_\beta - \dfrac{1}{L}E\left(\bar{i}_\beta\right) \end{cases} \quad (8)$$

To further suppress the chattering, we will change the boundary layer thickness of the hyperbolic tangent functions such that they vary with the change of rotation speed considering the stator voltage at the high-speed region is substantial compared to that at the low-speed region. This requires the inverter output voltage at SVPWM modulation to be large, which means the space voltage vector actuation duration should be lengthened. So in order to compensate for the time, the width of the boundary layer thickness should be broadened. Therefore, we have the hyperbolic tangent functions, which are defined as

$$\begin{bmatrix} E\left(\bar{i}_\alpha\right) \\ E\left(\bar{i}_\beta\right) \end{bmatrix} = k\omega_{ref} \begin{bmatrix} \dfrac{e^{\chi\bar{i}_\alpha} - e^{-\chi\bar{i}_\alpha}}{e^{\chi\bar{i}_\alpha} + e^{-\chi\bar{i}_\alpha}} \\ \dfrac{e^{\chi\bar{i}_\beta} - e^{-\chi\bar{i}_\beta}}{e^{\chi\bar{i}_\beta} + e^{-\chi\bar{i}_\beta}} \end{bmatrix} \quad (9)$$

where χ is a positive constant used to adjust the slope of the hyperbolic tangent functions, k and ω_{ref} represent the new sliding mode observer gain and the reference rotational velocity.

The corresponding curve is presented in Fig.2. It is shown that the gain k with the H function in the sliding mode switching surface can be adjusted easily by changing χ and ωref , thus the chattering is effectively weakened. The χ is adjusted to be the most appropriate value within the prescribed scope according to the demand change, which improves system robustness against dynamic uncertainties and attenuates disturbances on the system.

From the above equations, the EMF equations are expressed as follows

$$\begin{cases} \left(E\left(\bar{i}_\alpha\right)\right) \approx e_\alpha \\ \left(E\left(\bar{i}_\beta\right)\right) \approx e_\beta \end{cases} \quad (10)$$

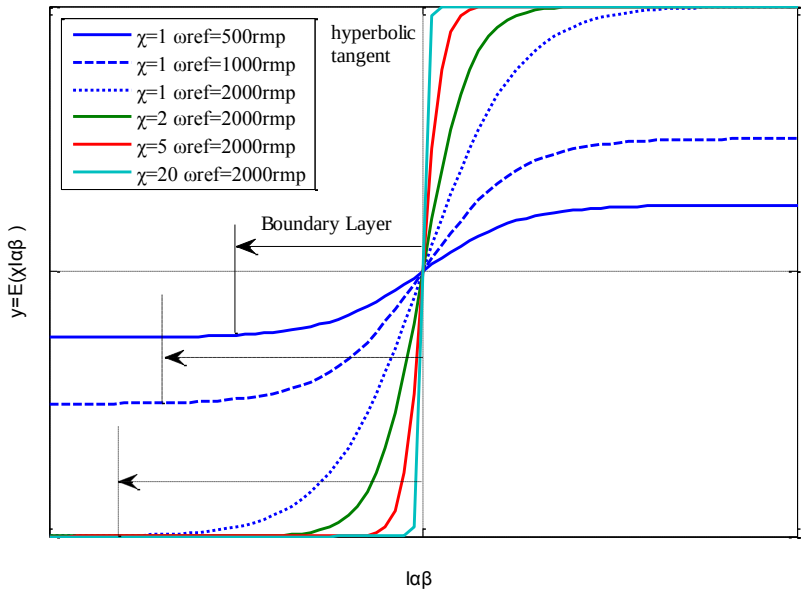

Figure 2. The curve with hyperbolic tangent functions

Because the motor angular velocity is far lower than the changing rate of current, if rotation speed keeps unchanged in a digital cycle, we can assume that $\dot{\omega}_r = 0$, combining (2), the EMF model can be expressed as

$$\begin{cases} \mathrm{d}e_\alpha / \mathrm{d}t = -\omega_r e_\beta \\ \mathrm{d}e_\beta / \mathrm{d}t = \omega_r e_\alpha \end{cases} \quad (11)$$

So in the EMF observer, the adaptive law for the rotor position and speed estimation can be expressed as

$$\begin{cases} \mathrm{d}\hat{e}_\alpha / \mathrm{d}t = -\hat{\omega}_r \hat{e}_\beta - h\bar{e}_\alpha \\ \mathrm{d}\hat{e}_\beta / \mathrm{d}t = \hat{\omega}_r \hat{e}_\alpha - h\bar{e}_\beta \\ \mathrm{d}\hat{\omega}_r / \mathrm{d}t = \bar{e}_\alpha \hat{e}_\beta - \bar{e}_\beta \hat{e}_\alpha . \end{cases} \quad (12)$$

where h is the observer gain, $\bar{e}_\alpha = \hat{e}_\alpha - e_\alpha$ and $\bar{e}_\beta = \hat{e}_\beta - e_\beta$.

Doing integral to (12), and combining it with (2), we have

$$\begin{cases} \sin\hat{\theta} = -\hat{e}_\alpha / \psi_f \hat{\omega}_r \\ \cos\hat{\theta} = \hat{e}_\beta / \psi_f \hat{\omega}_r \end{cases} \quad (13)$$

Namely,

$$\hat{\theta} = -\tan^{-1}\left(\frac{\hat{e}_\alpha}{\hat{e}_\beta}\right) \quad (14)$$

In order to prove its stability, we construct the Lyapunov function as follows

$$V=\frac{1}{2}\left(\bar{e}_\alpha^2+\bar{e}_\beta^2+\bar{\omega}_r^2\right) \quad (15)$$

From (12), we have

$$\begin{cases} \mathrm{d}\bar{e}_\alpha/\mathrm{d}t=-\hat{\omega}_r\hat{e}_\beta+\omega_r e_\beta-h\bar{e}_\alpha \\ \mathrm{d}\bar{e}_\beta/\mathrm{d}t=\hat{\omega}_r\hat{e}_\alpha-\omega_r e_\alpha-h\bar{e}_\beta \\ \mathrm{d}\bar{\omega}_r/\mathrm{d}t=\bar{e}_\alpha\hat{e}_\beta-\bar{e}_\beta\hat{e}_\alpha \end{cases} \quad (16)$$

Then considering (16), the derivative of (15) is obtained as

$$\dot{V}=\bar{e}_\alpha\dot{\bar{e}}_\alpha+\bar{e}_\beta\dot{\bar{e}}_\beta+\bar{\omega}_r\dot{\bar{\omega}}_r=-h(\bar{e}_\alpha^2+\bar{e}_\beta^2)\le 0 \quad (17)$$

It can be seen from the above equation that the stability of the rotor position estimation is only affected by h, independent of motor parameters.

b. SMO Stability and Resistance Estimation

The estimated phase currents are derived by subtracting (1) from (8), which can be represented as

$$\begin{cases} \dot{\bar{s}}_\alpha=\dot{\bar{i}}_\alpha=\dot{\hat{i}}_\alpha-\dot{i}_\alpha=-\frac{1}{L}\hat{i}_\alpha\bar{R}-\frac{R}{L}\bar{i}_\alpha+\frac{1}{L}e_\alpha-\frac{1}{L}E\left(\bar{i}_\alpha\right) \\ \dot{\bar{s}}_\beta=\dot{\bar{i}}_\beta=\dot{\hat{i}}_\beta-\dot{i}_\beta=-\frac{1}{L}\hat{i}_\beta\bar{R}-\frac{R}{L}\bar{i}_\beta+\frac{1}{L}e_\beta-\frac{1}{L}E\left(\bar{i}_\beta\right) \end{cases} \quad (18)$$

where $\bar{R}=\hat{R}-R$.

To verify the stability of the aforementioned SMO, the Lyapunov function is defined as

$$V=\frac{1}{2}S_n{}^TS_n+\frac{1}{2}\left(\hat{R}-R\right)^2 \quad V>0 \quad (19)$$

Differentiating (19), combining (18), we have

$$\dot{V}=S_n{}^T\dot{S}_n+\left(\hat{R}-R\right)\dot{\hat{R}}=\begin{bmatrix}\bar{i}_\alpha & \bar{i}_\beta\end{bmatrix}\begin{bmatrix}-\frac{1}{L}\hat{i}_\alpha\bar{R}-\frac{R}{L}\bar{i}_\alpha+\frac{1}{L}\left(e_\alpha-E\left(\bar{i}_\alpha\right)\right)\\ -\frac{1}{L}\hat{i}_\beta\bar{R}-\frac{R}{L}\bar{i}_\beta+\frac{1}{L}\left(e_\beta-E\left(\bar{i}_\beta\right)\right)\end{bmatrix}+\bar{R}\cdot\dot{\hat{R}}<0 \quad (20)$$

From the Lyapunov stability theorem [8], to satisfy the condition $\dot{V}<0$, we have

$$-\frac{1}{L}\left(\hat{R}-R\right)\begin{bmatrix}\bar{i}_\alpha & \bar{i}_\beta\end{bmatrix}\begin{bmatrix}\hat{i}_\alpha\\ \hat{i}_\beta\end{bmatrix}+\bar{R}\cdot\dot{\hat{R}}=0 \quad (21)$$

$$\begin{bmatrix}\bar{i}_\alpha & \bar{i}_\beta\end{bmatrix}\begin{bmatrix}-\frac{R}{L}\hat{i}_\alpha-\frac{R}{L}\left(\hat{i}_\alpha-i_\alpha\right)+\frac{1}{L}\left(e_\alpha-E\left(\bar{i}_\alpha\right)\right)\\ -\frac{R}{L}\hat{i}_\beta-\frac{R}{L}\left(\hat{i}_\beta-i_\beta\right)+\frac{1}{L}\left(e_\beta-E\left(\bar{i}_\beta\right)\right)\end{bmatrix}<0 \quad (22)$$

From (21), the stator resistance online identification can be defined as

$$\dot{\hat{R}} = \frac{1}{L}\left(\bar{i}_\alpha \cdot \hat{i}_\alpha + \bar{i}_\beta \cdot \hat{i}_\beta\right) \quad (23)$$

By combining (9) and (2), we have $\omega_{ref} = \frac{\sqrt{\hat{e}_\alpha{}^2 + \hat{e}_\beta{}^2}}{\psi_f}$, where $\varphi_f < 1$.

From (22-23), the observer gain can be expressed as

$$k\omega_{ref} \geq \max\left(|\hat{e}_\alpha|, |\hat{e}_\beta|\right) \quad (24)$$

So we can see $\dot{V} < 0$, and the asymptotical stability of the SMO is proved.

Fig.3 shows the block diagram of the adaptive SMO based on the hyperbolic tangent function with resistance online identification.

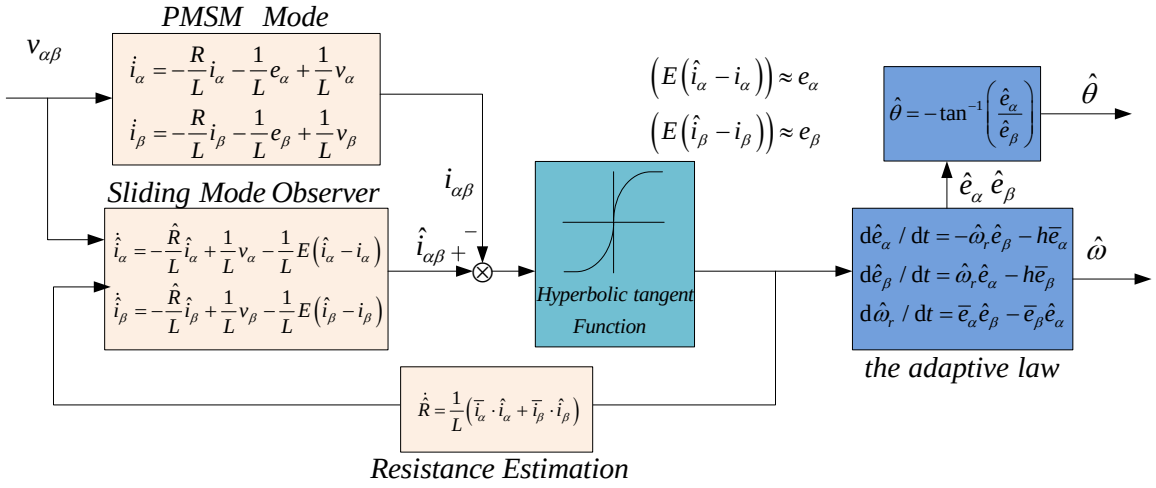

Figure 3. The block diagram of the adaptive SMO with resistance identification based on hyperbolic tangent function

Table 1:Units for magnetic properties

Symbol	Motor Parameters	Values and Units
P	Rated Power	100kw
T	Rated Torque	500n ṁ
v_r	Rated Speed	1900r/min
v_{max}	Maximum Speed	4000r/min
f_{sw}	Switching Frequency	4kHz
R	Stator Resistor	0.028Ω
L	Stator Inductor	0.365mH
J	Rotor Inertia	0.08kg ṁ^2
φ_f	Flux of PM	0.029Wb
p	Poles	4
k_{sw}	Sign function gain	500
k	Hyperbolic tangent function gain	1.1

IV. SIMULATION AND EXPERIMENTAL RESULTS

a. Simulation Result

To verify the performance of the proposed sliding mode observer, the whole PMSM drive control system was simulated in the MATLAB/SIMULINK environment. The motor parameters are shown in Table I. The whole control system uses vector control strategy, where the speed control loop and the current control loop simply adopt PI controllers. To show the performance of the developed observer, three different observers, the traditional SMO with sign function, and the adaptive SMO with hyperbolic tangent function without resistance identification, and the proposed adaptive SMO, will be compared. The vector control block diagram of the PMSM based on the adaptive SMO for electric vehicle propulsion system is illustrated in Fig.4.

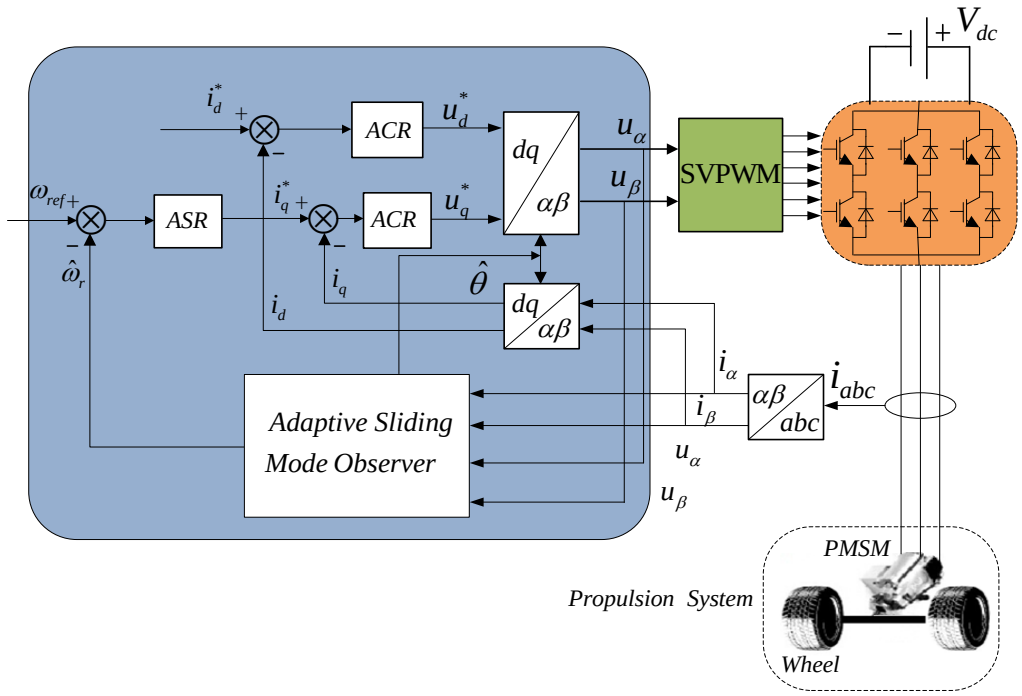

Figure 4. The vector control block diagram of the PMSM based on the adaptive SMO for electric vehicle propulsion system

The simulation results of three kinds of SMOs are shown in Fig.5-7. In the simulation, the reference speed steps up from 500 to 2000 r/min at 0.1s, the whole simulation time is 0.2s, the cut off frequency of first-order low-pass filter of traditional SMO is 1500 Hz, hyperbolic tangent

function parameter χ is 5. Considering stator resistance varied with motor temperature and resistance properties, so we assume $\Omega_T = 0.02\sin 20\pi t$ as a given resistance disturbance.

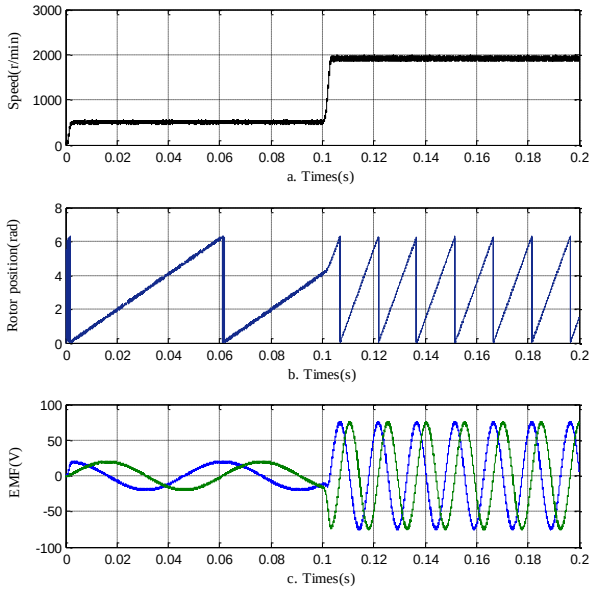

Figure 5. Simulation waveforms obtained by the conventional SMO using sign function. (a) Estimated speed. (b) Estimated rotor position. (c) Estimated EMF

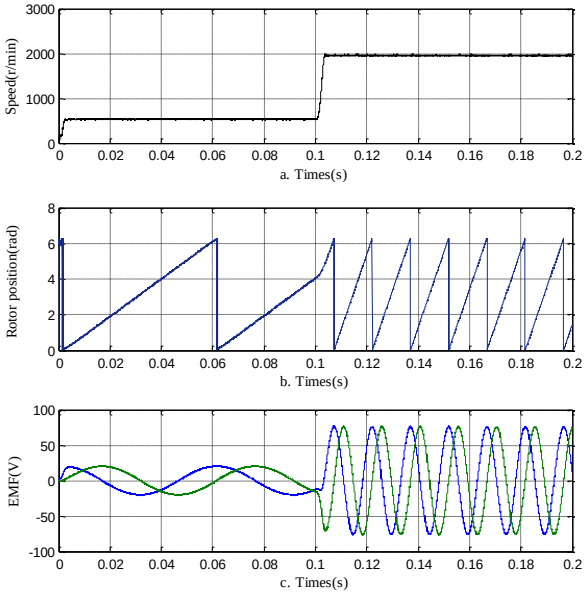

Figure 6. Simulation waveforms obtained by the adaptive SMO using a hyperbolic tangent function without resistance identification. (a) Estimated speed. (b) Estimated rotor position. (c) Estimated EMF

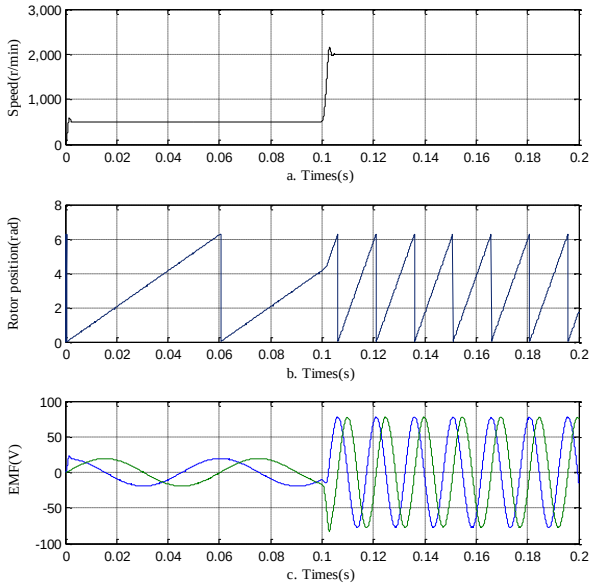

Figure 7. Simulation waveforms obtained by the adaptive SMO with resistance identification. (a) Estimated speed. (b) Estimated rotor position. (c) Estimated EMF

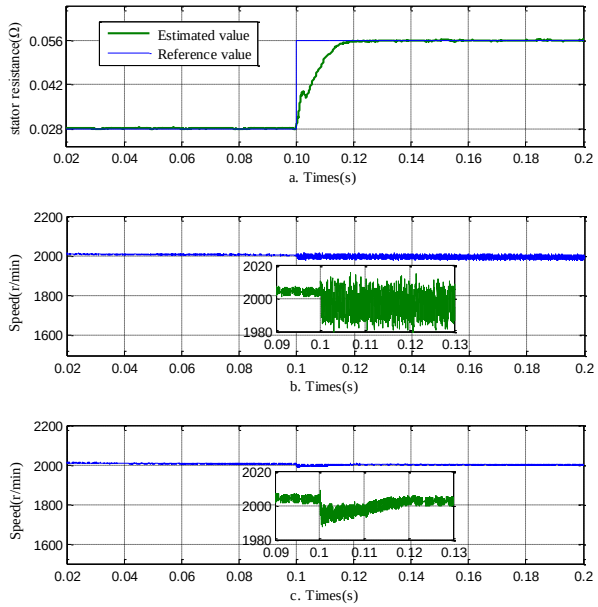

Figure 8. Simulation waveforms with the stator-resistance mutation. (a) Estimation of the changed resistance. (b) Velocity tracking without the resistance identification. (c) Velocity tracking with the resistance identification

Fig.5 shows the simulation waveforms obtained by the conventional method using a sign function. The chattering phenomenon, which appears in the estimated electromotive forces, seriously affects the accuracy of the estimated rotor position and speed.

Fig.6 shows the waveforms obtained by the adaptive SMO using a hyperbolic tangent function without resistance identification. Due to the use of the adaptive SMO observer, not only the low-pass filter and the phase compensation module are removed, but also the estimation accuracy is improved. We can come to the conclusion that the replacement of the switching function makes the chattering phenomenon significantly inhibited and the estimation precision has been improved to a certain extent by comparing the above shown results.

Fig.7 displays the simulation waveforms obtained by the adaptive SMO with resistance identification. The simulation results indicate that the chattering phenomenon can be further reduced by adding the resistance identification loop, and the errors of the estimated rotor position and speed are nearly eliminated.

It is noted that in the above shown graphs, the reference speed is changed from 500 to 2000 r/min at 0.1s. With the increase of rotation speed, EMF variation ranges in Fig.5 have been increased. However, due to the conventional SMO gain does not change accordingly, the sign function of boundary layer thickness also remains the same. Thus the steady-state error at low speed is further intensified while running at a high speed. So is the chattering phenomenon. In Figs.6 and 7, the boundary layers are changed according to the rotation speed, which can effectively weaken the chattering phenomenon and strengthen the robustness of the system especially in high speed running stage. In Fig.7, the chattering is eliminated thoroughly. Meanwhile, to test the performance of this resistance identification algorithm, we design another simulation experiment with the stator-resistance mutation. The resistance value steps up from 0.028 to 0.056 at 0.1s. The reference speed is 2000 r/min.

Fig.8a shows the new SMO can quickly estimate the changed resistance in 0.03s within 2% error range and can update in real-time to reduce the rotation speed chattering caused by the change of electrical resistance. Fig.8b shows the velocity tracking results without the resistance identification, the speed oscillation is aggravated by the changed resistance, while Fig.8c shows that the proposed resistance identification recovers rotation speed in 0.03s.

b. Experimental Results

With using the previously designed observer, the ground experiments are conducted on a platform based on PMSM in an electric vehicle traction system. The control system hardware uses high-speed DSP processor (TMS320F2812) and FPGA as the core devices and is based on

the fast bus technology. The system can achieve the function such as high-performance vector control, model optimization, automatic parameter identification functions. Technical performance parameters of the PMSM used in the experiment are listed in the Table I. The experimental platform is presented in Fig.9.

Figure 9. The experimental platform

Fig.10 shows the waveforms of the back electromotive force estimation and rotor position estimation by a traditional sliding-mode observer and the adaptive sliding-mode observer, respectively. As shown in the figure, the adaptive sliding-mode observer can eliminate the buffeting obviously and identify the rotor position more accurately. In order to verify the dynamic response of the new algorithm, the torque step and speed step experiments are conducted with the newly developed sliding-mode observer.

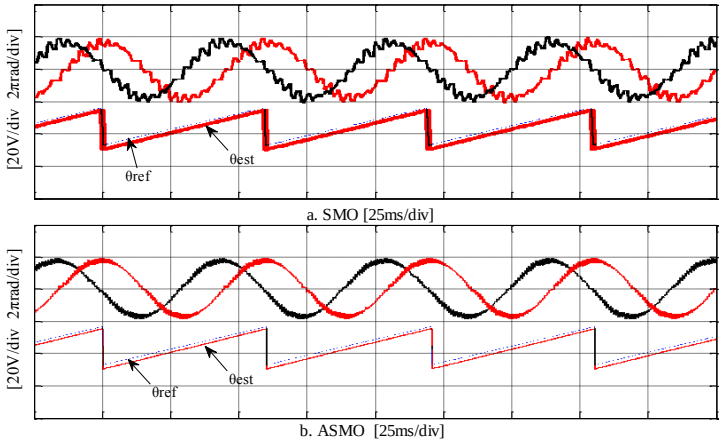

Figure 10. Waveforms of the back electromotive force estimation (e_α and e_β) and rotator position identification at 500 r/min. (a) SMO using sign function. (b) Adaptive SMO using a hyperbolic tangent function

Fig.11 is waveforms of current, the rotor position and speed when the range of speed step is 1000 to 2000 r/min. Fig.12 are waveforms of the current and rotor position identification corresponding to the motor torque of step change at 100 r/min and 1000 r/min respectively, As shown in these figures, the accuracy of the rotor position identification at high speed is still high and the position estimation is not affected in the step response. Experimental results show that the new adaptive SMO can effectively achieve the position estimation without a position sensor in the whole speed range. Chattering is greatly declined and the accuracy is improved to some extent compared with the conventional slide-mode observer.

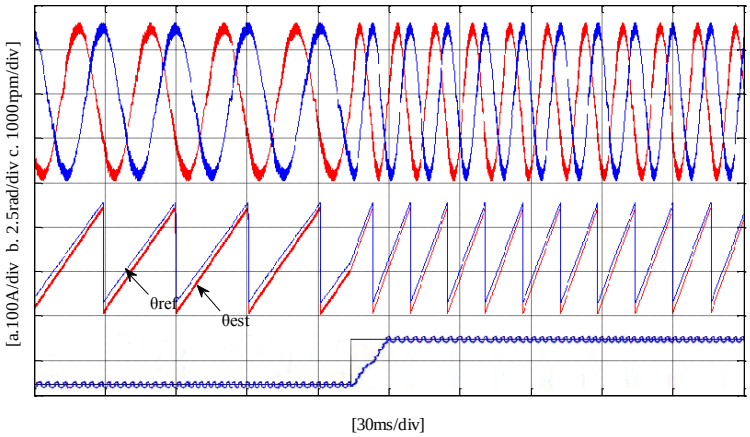

Figure 11. Waveforms of the rotor position, speed and phase stator current when the range of speed step is 1000 to 2000 r/min. (a) i_a and i_b. (b) The reference position and estimated position. (c) The reference speed and estimated speed

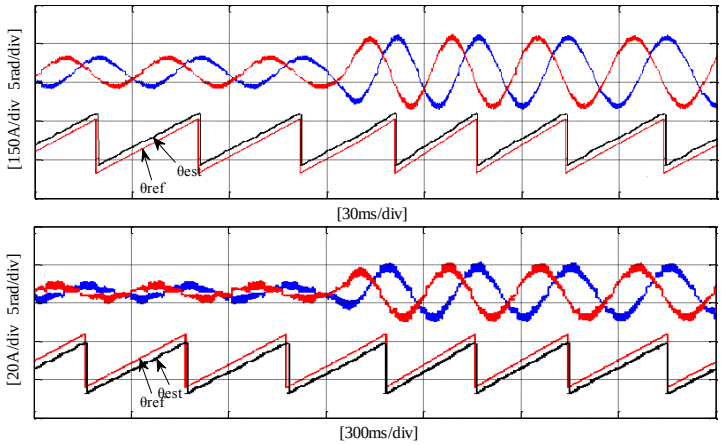

Figure 12 Waveforms of the phase stator current (i_a and i_b) and rotor position (The reference position and estimated position) identification with the motor torque of step change. (a) at 1000r/min (b) at 100r/min.

V. CONCLUSIONS

In this paper an adaptive sliding-mode observer with resistance estimation has been proposed for PMSM sensorless control in electric vehicles drive system. The stability of the new adaptive SMO is proved by Lyapunov stability analysis. The sign functions are replaced by the hyperbolic tangent functions with variable boundary layer thickness to weaken the chattering. An new adaptive law for rotor position and speed estimation is designed by the new SMO convergence condition to eliminate the low-pass filter and phase compensation module and to reinforce dynamic performance and the robustness of system. The stator-resistance identification is raised to further strengthen the robustness of the system. Simulation and experimental results show that the new SMO achieves better performance than the conventional SMO observer.

VI. AKNOWLEDGEMENT

This research was supported under the National Key Technology Research and Development Program of the Ministry of Science and Technology of China (2012BAF09B02).

REFERENCES

[1] Azuma, Takehito, "Design and experimental verification of state predictive LQG controllers for networked control systems", The International Journal on Smart Sensing and Intelligent Systems, Vol. 3, No.7, 2014, pp. 1201-1220.

[2] J.J.Hu, H. Morais and T. Sousa, "Electric vehicle fleet management in smart grids: A review of services, optimization and control aspects", Renewable and Sustainable Energy Reviews, vol. 56, pp. 1207-1226, Apr. 2016.

[3] Tie SF and Tan CW, "A review of energy sources and energy management system in electric vehicles", Renewable Sustainable Energy Rev., vol. 20, pp. 82-102, Apr. 2013.

[4] J. B. Wang, X. B. Yuan and Atallah. K, "Design Optimization of a Surface-Mounted Permanent-Magnet Motor with Concentrated Windings for Electric Vehicle Applications", IEEE Transactions on Vehicular Technology, vol. 62, no. 3, pp. 1053-1064, Mar. 2013.

[5] R. D. Jorge, A. N and A. M. Marco, "Digital Sliding-Mode Sensorless Control for Surface-Mounted PMSM", IEEE Transactions on Industrial Informatics, vol. 10, no. 1, pp.137-151, Feb. 2014.

[6] M.Pacas, "Sensorless drives in industrial applications", IEEE Ind. Electron. Mag., vol. 5, no. 2, pp. 16-23, June 2011.

[7] R. M. Caporal, E. Bonilla-Huerta, M.A. Arjona and C. Hernandez, "Sensorless Predictive DTC of a Surface-Mounted Permanent-Magnet Synchronous Machine Based on Its Magnetic Anisotropy", IEEE Transactions on Industrial Electronics, vol. 60, no. 8, pp. 3016-3024, Aug. 2013.

[8] Z. Wang, K. Lu and F. Blaabjerg, "A simple startup strategy based on current regulation for back-EMF based sensorless control of PMSM", IEEE Transactions on Power Electronics, vol. 27, no. 8, pp.3817-3825, Aug. 2012.

[9] M. Naidu and B. K. Bose, "Rotor position estimation scheme of a permanent magnet synchronous machine for high performance variable speed drive", in IEEE Industry Applications Society Annual Meeting，Houston, 1992, pp. 48-53.

[10] C. French and P. Acarnley, "Control of permanent magnet motor drives using a new position estimation technique", IEEE Transactions on Industry Applications, vol. 32, no. 5, pp. 1089-1097, Sep. 1996.

[11] S. M. Jung , J. S. Park , H. W. Kim , K. Y. Cho and M. J. Youn, "An MRAS-based diagnosis of open-circuit fault in PWM voltage-source inverters for PM synchronous motor drive systems", IEEE Transactions on Power Electronics, vol. 28, no. 5, pp.2514-2526, May 2013.

[12] A. Piippo, M. Hinkkanen and J. Luomi, "Analysis of an adaptive observer for sensorless control of interior permanent magnet synchronous motors", IEEE Transactions on Industrial Electronics, vol. 55, no. 2, pp. 570-576, Feb. 2008.

[13] A. M. Alshawish, R. Ahmadi, "An optimization based method for design of the adaptive mechanism parameters in a model adaptive reference system estimator in a sensorless motor drive system", IEEE Transactions on Power and Energy Conference at Illinois (PECI), pp. 1-5, Feb. 2015.

[14] Ying Zhu, Ming Cheng, Wei Hua and B.F. Zhang, "Sensorless Control Strategy of Electrical Variable Transmission Machines for Wind Energy Conversion Systems", IEEE Transactions on Magnetics, vol. 49, no. 7, pp. 3383-3386, July 2013.

[15] A. Accetta, M. Cirrincione, M. Pucci and G. Vitale, "Sensorless control of PMSM fractional horsepower drives by signal injection and neural adaptive-band filtering", IEEE Transactions on Industrial Electronics, vol. 59, no. 3, pp. 1355-1366, Mar. 2012.

[16] S. Bolognani, R. Petrella, A. Prearo and L. Sgarbossa, "Automatic tracking of MTPA trajectory in IPM motor based on AC current injection", IEEE Transactions on Industry Applications, vol. 47, no. 1, pp. 105-114, Feb. 2011.

[17] M. Slimane and D. Diallo, "PMSM Drive Position Estimation: Contribution to the High-Frequency Injection Voltage Selection Issue", IEEE Transactions on Energy Conversion, vol. 30, no. 1, pp.349-358, Mar. 2015.

[18] Z. Q. Zhu and L. M. Gong, "Investigation of effectiveness of sensorless operation in carrier-signal-injection-based sensorless control methods", IEEE Transactions on Industrial Electronics, vol. 58, no. 8, pp. 3431-3439, Aug. 2011.

[19] J. Hu, J. Liu and L. Xu, "Eddy current effects on rotor position estimation and magnetic pole identification of PMSM at zero and low speeds", IEEE Transactions on Power Electronics, vol. 23, no. 5, pp.2565-2575,Sept. 2008.

[20] R.S. Muñoz Aguilar, A. Dòria-Cerezo, E. Fossas and R. Cardoner, "Sliding mode control of a stand-alone wound rotor synchronous generator", IEEE Transactions on Industrial Electronics, Vol. 58 , No. 10, pp. 4888-4897, Oct. 2011.

[21] B. Jin and C. Y. Sun, "Research on lateral stability of four hubmotor-in-wheels drive electric vehicle", The International Journal on Smart Sensing and Intelligent Systems, vol. 8, no. 3, pp.1855-1875, Sep. 2015.

[22] S. Po-ngam and S. Sangwongwanich, "Stability and dynamic performance improvement of adaptive full-order observer for sensorless PMSM drive", IEEE Transactions on Power Electronics, vol. 27, no. 2, pp. 588-600, Feb. 2012.

[23] A. M. Yazdani, A. Ahmadi and S. Buyamin, "Imperialist competitive algorithm-based fuzzy PID control methodology for speed tracking enhancement of stepper motor", International Journal on Smart Sensing and Intelligent Systems, vol. 5, No. 3, 2012, pp. 717-741.

[24] W.Q. Zhao, T. Shi, Y. Wang and Y. Yan, "New Sliding-Mode Observer for Position Sensorless Control of Permanent-Magnet Synchronous Motor", IEEE Transactions on Industrial Electronics, vol. 60, no. 2, pp. 710-719, Feb. 2013.

[25] K. Hongryel, S. Jubum and L. Jangmyung, "A High-Speed Sliding-Mode Observer for the Sensorless Speed Control of a PMSM", IEEE Transactions on Industrial Electronics, vol. 58, no. 9, pp. 4069-4077, Sept. 2011.

[26] G. Tarchala, "Influence of the sign function approximation form on performance of the sliding-mode speed observer for induction motor drive", in Proc. IEEE Int. Sym. Ind. Electron, Gdansk, 1985, pp. 1397-1402.

[27] B. Oscar, A. Patxi and M. Jose, "A real-time estimation and control scheme for induction", Journal of the Franklin Institute, vol. 351, no. 8, pp. 4251-4270, Aug. 2014.

[28] W. C. Chi, M. Y. Cheng, "Implementation of a sliding-mode-based position sensorless drive for high-speed micro permanent-magnet synchronous motors", ISA Transactions, vol. 53, no. 2, pp. 444-453, Mar. 2014.

[29] F. Plestan, A. Glumineau and S. Laghrouche, "A new algorithm for high order sliding mode control", International Journal of Robust and Nonlinear Control, vol. 18, no. 4, pp. 441-453, Mar. 2008.

[30] Reza, C.M.F.S., Islam, Didarul and Mekhilef, "Modeling and Experimental Verification of ANN Based Online Stator Resistance Estimation in DTC-IM Drive", Journal of Electrical Engineering and Technology, vol. 9, no. 2, pp.550-558, Mar. 2014.

[31] E. Shehata, "Speed sensorless torque control of an IPMSM drive with online stator resistance estimation using reduced order EKF", International Journal of Electrical Power & Energy Systems, vol. 47, pp. 378-386, May 2013.

[32] B.A. Hechmi, J. Mohamed, B. Mohamed and G. Moncef, "High performance sensorless speed vector control of SPIM Drives with on-line stator resistance estimation", Simulation Modelling Practice and Theory, vol. 19, no. 1, pp. 271-282, Jan. 2011.

[33] R. Habib-ur, D. Rached, "A fuzzy learning-Sliding mode controller for direct field-oriented induction machines", Neurocomputing, vol. 71, no. 13, pp. 2693-2701, Aug. 2008.